International Journal of Pharmacology

ISSN 1811-7775

science alert

ansinet
Asian Network for Scientific Information

OPEN ACCESS International Journal of Pharmacology

ISSN 1811-7775
DOI: 10.3923/ijp.2024.305.317

Research Article
Potential Protective Effect of Agmatine on Bleomycin-Induced Pulmonary Fibrosis in Male Albino Rats

Khlood Mohammed Mehdar

Department of Anatomy, College of Medicine, Najran University, Najran, Saudi Arabia

Abstract

Background and Objective: Pulmonary fibrosis (PF) etiology remains unclear with limited therapeutic options. Uncontrolled lung fibroblast proliferation produces excessive ECM proteins, leading to fibrosis. This study explores the protective effect of Agmatine (agma) and pirfenidone (PFD) on BLM-induced pulmonary fibrosis in rats. **Materials and Methods:** About 30 male adult Sprague-Dawley albino rats 6-8 weeks old, weighing 200±25 g were divided into five groups: Control group, BLM group, BLM+PFD group, BLM+agma group and BLM+PFD+agma group. Finally, all animals were sacrificed after 28 days. Lung samples were obtained for histological, immunohistochemical and biochemical studies. Data were statistically analyzed One-way Analysis of Variance (ANOVA) followed by the *post hoc* Tukey's test. **Results:** The study found that BLM treatment led to decreased SOD and GSH levels and increased HGMB1 and MDA levels. However, treatment with PFD, agma and PFD+agma resulted in lower HMGP1 and MDA levels and higher SOD and GSH levels. Agma treatment helped to restore the standard epithelial lining of the bronchi and alveoli. The BLM+PFD and BLM+Agmatine groups had reduced interalveolar septa thickness, while the BLM+PFD+Agmatine group showed a significant decrease in the mean surface area of alveolar space and location of collagen fibers. **Conclusion:** Agmatine, combined with PFD, was shown to reduce the severity of BLM-induced histological and biochemical alterations in rat lungs without completely reversing them. Possible explanations include agma's ability to reduce inflammation, act as an antioxidant and mop up free radicals. These findings can be of value for future clinical applications.

Key words: Agmatine, bleomycin, pulmonary fibrosis, albino rats, histological, immunohistochemical, oxidative stress, HGMB1

Citation: Mehdar, K.M., 2024. Potential protective effect of Agmatine on bleomycin-induced pulmonary fibrosis in male albino rats. Int. J. Pharmacol., 20: 305-317.

Corresponding Author: Khlood Mohammed Mehdar, Department of Anatomy, College of Medicine, Najran University, Najran, Saudi Arabia

Competing Interest: The author has declared that no competing interest exists.

Data Availability: All relevant data are within the paper and its supporting information files.

INTRODUCTION

A fatal lung disease that worsens over time, pulmonary fibrosis (PF) is a serious threat. It's the final step of many different lung inflammatory diseases. Pulmonary fibrosis is distinguished by the deterioration of the alveolar organization. The accumulation of myofibroblasts, the remodelling of the lung parenchyma and the deposition of an excessive amount of extracellular matrix[1]. Common interstitial lung disorders include PF, an irreversible, deadly lung disease with a median survival span of fewer than three years[2]. Emerging research has demonstrated that certain types of cells and cytokines play crucial roles in the progression of PF, even if the etiology of PF remains unknown[3].

Anti-fibrinolytic components, glucocorticoids and antioxidants are only a few of the treatments shown to be successful in both animal and human PF research. Medications like glucocorticoids and immunosuppressive drugs can help improve patients' prognoses, but they come with serious drawbacks and often aren't effective enough to warrant their use[4]. There are currently just two medications approved by Food and Drug Administration (FDA), they are, nintedanib and pirfenidone (PFD). Pirfenidone has demonstrated significant protective effects against fibrosis in a study conducted on rats with bleomycin-induced pleuritis and fibrosis[5]. The PFD alleviates pulmonary fibrosis by employing various molecular mechanisms, such as suppressing TGF-β signaling to decrease fibroblast activation and collagen synthesis. Additionally, it modulates cytokines and growth factors implicated in fibrosis progression. Furthermore, it possesses anti-inflammatory properties that inhibit immune cell activation and inflammation, along with antioxidant attributes that combat oxidative stress and safeguard lung tissue. Moreover, it regulates the remodeling of the extracellular matrix, thereby preventing excessive collagen accumulation[5]. The antifibrotic agents pirfenidone and nintedanib have been agreed and utilized for a broad duration in the treatment of elderly patients suffering from idiopathic pulmonary fibrosis. Real-world data has confirmed that this particular group exhibit commendable tolerability, compliance and a manageable side effect profile when administered these medications[6]. Although these medications slow PF's course and improve patients' quality of life, they have not been found to significantly lower fatality rates[7]. Thus, there is an ongoing critical need for research into and development of novel potential targets and treatments to limit PF.

A common chemotherapeutic drug used to treat a variety of carcinomas is bleomycin (BLM). Because pulmonary toxicity is BLM's most serious side effect, it is routinely cited as one of the most extensively utilized drugs for inducing experimental lung fibrosis[4,8]. It is theorized that BLM initiates inflammatory and fibro-proliferative responses by inducing reactive oxygen species (ROS), which bind to DNA and cause DNA damage. In addition, because BLM contributes to the loss of natural antioxidant defenses, it has been associated with an amplification of oxidant-mediated tissue harm[9,10].

High-Mobility Group Box 1 (HMGB1) is an inflammatory and dangerous signal that has been demonstrated the ability to directly enhance the growth of fibroblasts and trigger epithelial-mesenchymal transition (EMT), which is a vital process in acquiring certain characteristics of mesenchymal cell power by alveolar epithelial cells (including ECM-producing cells myofibroblasts) and promote the production of ECM proteins[11-13]. In light of this, anti-HMGB1 drugs may provide a promising strategy for preventing PF.

As a key biogenic amine, Agmatine (4-aminobutyl) guanidine finds widespread use in industries as diverse as pharmaceuticals, food, chemicals and animal feed. Medical professionals are interested in agma because of its potential to improve metabolic rate, maintain nutritional equilibrium and speed up the body's healing process[14-16]. In addition, several researchers investigated agma's antioxidant, anti-inflammatory and anti-apoptotic properties to determine whether or not they may be used to protect neurons. As a result, it holds great promise as a medication for managing a wide range of neurological conditions[17-20].

Previous study has shown that agma can mitigate acute-zymosan on mice and nicotine-induced pulmonary damage in rats, as it has been shown to have anti-inflammatory and anti-oxidant properties[21]. Agmatine's effects on pulmonary fibrosis are still undetermined though. Therefore, this study aims to investigate the protective effects of agma alone or in combination with pirfenidone (PFD) against bleomycin-induced pulmonary fibrosis in rats.

MATERIALS AND METHODS

Study area: The study conducted at the animal facilities of King Fahd Medical Research Center's Animal House, Faculty of Medicine, King Abdul-Aziz University, Jeddah, Saudi Arabia. The study were conducted from March 2023 to September 2023.

Drugs: Bleomycin (BLM) was purchased from Nippon Kayaku Co. (Ltd., Tokyo, Japan). Pirfenidone (Esbriet) (brand name: Pirfenex Cipla® Capsule 200 mg) and Agmatine (Merck, S7127, Merck KGaA, Darmstadt, Germany) white powder dissolved in normal saline.

Animals: Thirty adult male Sprague-Dawley albino rats, 6-8 weeks old, weighing 200±25 g, were purchased from the Animal House of King Abdul-Aziz University (KAU) Pharmacy Faculty in Jeddah, Saudi Arabia. Standard animal cages (five rats per cage) were used and a constant room temperature (23±1°C), light/dark cycle (12 hrs on, 12 hrs off) and humidity level (55±5%) were maintained throughout the duration of the study. Rat chow and water were provided *ad libitum* and they had unrestricted access to food.

Ethical consideration: Ethical approval for this work was obtained from the Institution's Bioethics and Research Committee under the reference number (No.: 010252-022515-DS).

Induction of pulmonary fibrosis: Anesthetize rats using a combination of ketamine/xylazine and inject 200 µL intraperitoneally of ketamine/xylazine solution[22] using a 1 mL syringe with 26½ G needle. Bleomycin dissolved in normal saline was used to induce PF in rats. The rats were anaesthetized and given an intratracheal instillation of 5 mg/kg bleomycin hydrochloride for injection (at a concentration of 5 mg/mL, with an injection of 1 mL/kg volume) using a 1 mL syringe. Suspend the rat from the loop of surgical thread between the upper incisors while it is on the operating table. Make sure there is enough light to see the vocal cords. To see the vocal cords, gently pull and extend the tongue to one side with sterile padded forceps toward the mandible. Next, place the pipet tip containing the bleomycin solution towards the rear of the oral cavity and release it into the back of the mouth during inspiration. The liquid is delivered through the endotracheal tube when there is a gasp. The BLM solution is substituted with a similar amount of sterile PBS for the control animals. Pull the top incisors free of the suspension thread and relax the tongue. Until the rat fully recovers from the anaesthetic, keep it warm by placing it beneath a heating lamp or pad[22].

Experimental design:

- Control group (n = 6): From day 2, rats received daily oral gavages of the vehicle after receiving intratracheal instillations of a volume equivalent to normal saline instead of BLM
- The BLM group (n = 6): One dose of BLM was given to the rats and then they were given vehicle through oral gavage daily from the second day for the rest of the experiment[22]
- The BLM group treated with PFD (BLM+PFD) (n = 6): The administered dose of PFD was adapted from the work of Song *et al.*[23] from the second day following modeling, PFD (50 mg/kg) was orally administered once daily to rats in PFD-treated groups via gastric gavage
- The BLM group treated with agma (BLM+agma) (n = 6): This group had an endotracheal infusion of BLM, followed by agma treatment. Agma (10 mg/kg) was given intra-peritoneally once daily, to Agmatine-treated groups of rats beginning on day 2 post-modelling. The administered dose of Agmatine was adapted from the work of El-Agamy *et al.*[21]
- The BLM treated with agma and PFD (BLM+Agmatine+PFD) (n = 6): BLM is instilled endotracheal and then this group was treated by a combination of Agmatine and PFD at the same previous doses

After 28 days, the rats were injected intraperitoneally with sodium pentobarbital (50 mg/kg) to induce anaesthesia and then they were exsanguinated to collect lung tissue. A portion of each rat's left lung was removed and homogenized in cold saline to create a 10% lung homogenate. The BCA protein detection kit was used to measure the protein concentration in the supernatant collected after centrifugation at 1500 g for 10 min (Beyotime, Shanghai, China). Paraffin sections were made for histological analysis after the right lung was removed.

Histological examination: Light microscopic examination of lung tissue embedded in paraffin blocks preserved in 10% formol saline was performed. Haematoxylin and Eosin (H&E) staining was used for more comprehensive histological analysis, whereas Masson trichrome was used to identify collagen fibers in sections that were 5-6 m thick. Under a light microscope (Olympus BX51 microscope, Tokyo, Japan), the specimen section was observed and photographed.

Enzyme-linked immunosorbent assay for rat High Mobility Group Protein B1 (HMGB1) and the oxidative stress markers malondialdehyde[14], superoxide dismutase (SOD) and reduced glutathione[24]: The level of HMGB1 in the rats' lungs was determined by Enzyme-Linked Immunosorbent Assay (ELISA). The HGMB1 content in the lung homogenate supernatant was measured according to the method described by Yamada *et al.*[25] using a commercial kit purchased from MyBioSource (San Diego, California, United States, Cat. No: MBS703437).

Lung malondialdehyde[14] levels were measured to evaluate lipid peroxidation. Using a commercial kit acquired from MyBioSource (San Diego, California, United States, Cat. No: MBS268427), we determined the MDA concentration in the lung homogenate supernatant in accordance with the protocol reported by Satoh[26]. The evaluation of superoxide dismutase (SOD) activity was conducted using the method outlined by Nishikimi *et al.*[27] using a commercial kit purchased from MyBioSource (San Diego, California, United States, Cat. No: MBS036924). The concentration of reduced glutathione[26] in the lung homogenate was determined by means of the described method by Giustarini *et al.*[28] using a commercial kit purchased from MyBioSource (San Diego, California, United States, Cat No. MBS265966).

Morphometric analysis: Each group of rats (n = 6) had ten non-overlapping fields measured to determine the following: The mean thickness of the interalveolar septa in (μm), the mean alveolar space surface area in (μm^2) of H&E-stained sections[29] and the area percent of collagen fibers in Masson trichrome stain[30]. Digimizer image analysis software (MedCalc Software bvba, Belgium) was used to take the measurements from ×40 photomicrographs. The NIH's ImageJ (version 1.50) was used to quantify them.

Statistical analysis: The SPSS software was utilized to analyze the data obtained from the Digimizer image analyzer and biochemical data (Statistical Package for the Social Sciences) program version 26 (IBM, Armonk, New York, USA). One-way Analysis of Variance (ANOVA) was used to compare the control and experimental groups and the *post hoc* Tukey's test was used to determine statistical significance. Differences were graded as significant if $p<0.05$. GraphPad Prism 9 (San Diego, California, USA) was used to create the graphs.

RESULTS

Histological results

Haematoxylin and Eosin (H&E) stained sections: The alveoli in the control group's lung sections seemed patent and the interalveolar septa were thin. The bronchioles exhibited a lining of simple columnar ciliated epithelium over folded mucosa. Thin rims of lamina propria and simple squamous epithelium lined the alveolar sacs and alveoli. Pneumocytes of both types (type I and type II) contributed to the alveolar epithelium. Pneumocytes of type I were narrow and had little cytoplasm and flattened nuclei. The shape of type II pneumocytes appeared to be either spherical or cuboidal, exhibiting large, rounded nuclei and cytoplasm filled with vacuoles. Commonly found in the angular regions of alveolar septa, these epithelial protrusions had a rounded apical surface that rose above the level of the surrounding epithelium. A thin layer of alveolar epithelia, capillaries and delicate connective tissue were between the alveoli. Divisions of pulmonary arteries and veins were in interstitial lung tissue (Fig. 1a).

The BLM group showed vacuolated cytoplasm, pyknotic nuclei in the epithelial lining of the bronchiolar passageways and accumulated eosinophilic red material in the interstitial tissue. It is important to take note of the red blood cell (RBC) extravasations and the extensive cellular infiltration in the thickened interalveolar septa surrounding the alveoli. Many alveoli were completely wiped off and others had collapsed or had their lumens widened. In most stained sections, we see enormous, dilated blood vessels constricted at the center and have thicker walls. Red blood cell extravasations and eosinophilic exudates were common in the inter-alveolar septa. Much red blood cell (RBC) extravasations and acidophilic structures were observed close to the inflammatory cells in some sections (Fig. 1b). Lung architecture improved in the BLM group treated with PFD (BLM+PFD), but not to the point of full histological recovery. Lung tissue sections showed moderate thickening of septa and few inflammatory cell infiltrations in the thinnest parts of the blood vessel wall. Note how the alveoli look like the control group (Fig. 1c). Lung structure was improved in BLM treated with agma alone (BLM+Agmatine). Near the bronchi, researchers spotted a scattering of cells indicating inflammation, but these spots were rather small. Also, the epithelium lining the bronchi was similar to that of the healthy controls. Take note of how most alveoli are visible with narrow inter-alveolar septa, almost identical to the control group (Fig. 1d). Interestingly, BLM treated with the lung tissues exhibited a significant improvement in both the PFD and agma groups. The integrity of the lung alveoli, blood vessels and bronchioles remained relatively similar to that of the control group (Fig. 1e).

Masson's trichrome stain: Control group rat lung sections examined showed low collagen fiber density in perivascular regions. Interalveolar septa and bronchioles had very few collagen fibers (Fig. 2a). Collagen fibers appeared to be more pronounced in the BLM group (a sign of lung fibrosis) than in the control group (Fig. 2b). In contrast, collagen fibers appeared to be reduced in the interalveolar septa and the bronchial mucosa of BLM+PFD sections (Fig. 2c) and in the BLM+Agmatine sections (Fig. 2d). Furthermore, in BLM+PFD+Agmatine, not many collagen fibers were visible in the interalveolar septa or along the bronchial wall (Fig. 2e).

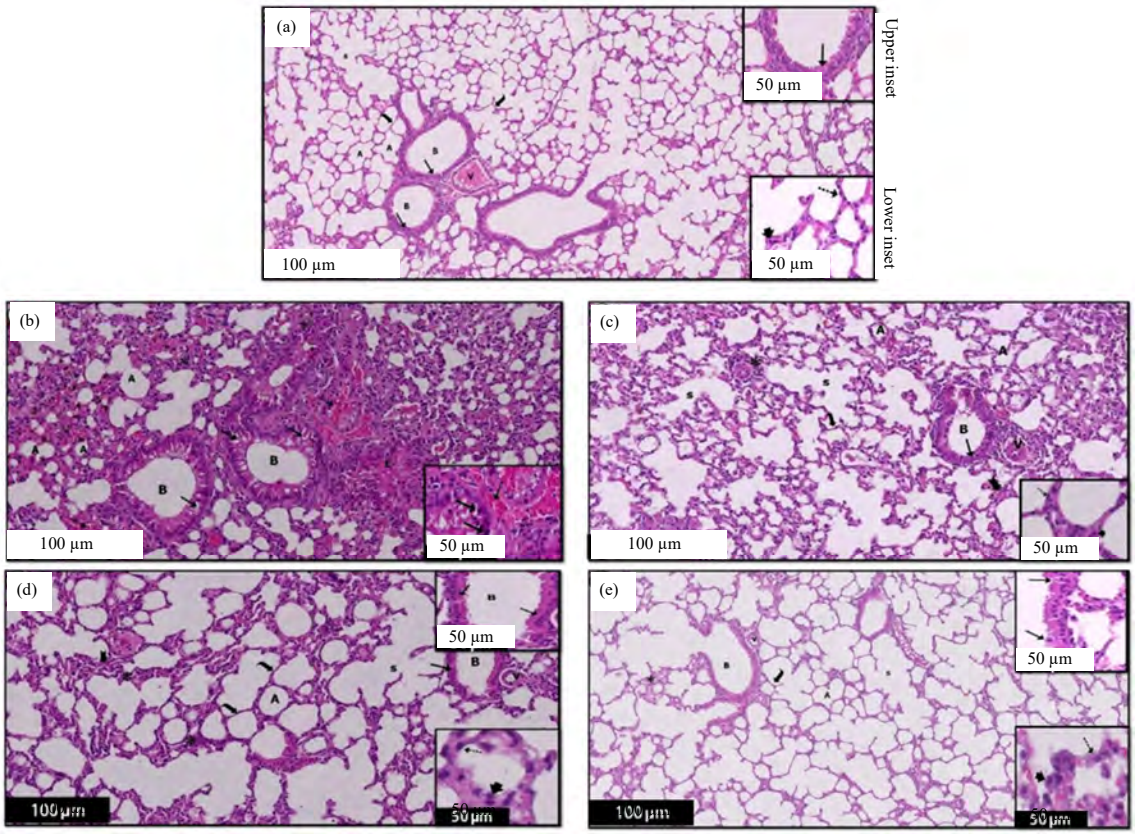

Fig. 1(a-e): A section of a rat lung in different experimental groups after 28 days showing, (a) Control group: The image shows the typical structure of a lung, (b) Bleomycin group: The image depicted the lung tissue exhibits a prominent loss of bronchiole architecture (B) and inflammation (*) within the interstitial tissue, (c) Bleomycin+pirfenidone (PFD): The control group showed a moderate improvement in lung architecture, but did not achieve complete histological recovery in comparison to the control group, (d) Bleomycin+agma: Most of the bronchiolar (B) epithelial lining is normal compared to the BLM and PFD-treated group and (e) Bleomycin+PFD+agma

(a) where the air sacs (A) and alveolar sacs (s) are expanded, and they are separated by thin walls (curved arrow). Additionally, the lung contains bronchioles (B) located near blood vessels (v). The bronchioles (B) have a partially ciliated, simple columnar epithelium (upper inset). On the other hand, the air sacs (A) are elongated, and their thin walls are lined with flat-nuclei pneumocytes type I (dot arrow) and rounded-nuclei cuboidal pneumocytes type II (arrowhead) (lower inset). These cells project towards the air sacs (A), (b) The majority of the alveoli are obliterated, with some being collapsed and others widened (A). Additionally, the presence of marked eosinophilic exudate (E) and multiple extravasations of RBCs (dot arrow) is evident. The lower inset of the image reveals the bronchiolar passage's lumen (B), It appears that the epithelial lining is vacuolated and the nuclei are darkly stained (↑). Furthermore, there are several extravasations of RBCs (dot ↑) visible, (c) The lung tissue exhibits some bronchioles with vacuolated epithelial cells (↑) alongside normal lining epithelium. There is moderate inflammatory cell infiltration (*) in the moderately thickened septa (bifid arrow), around alveoli and bronchioles, and thickened blood vessels wall (v). The majority of the alveoli are almost as apparent as the control group, with thin pneumocytes type I (dot arrow) and cuboidal pneumocytes type II (arrowhead) with rounded nuclei projecting to the alveoli lumen (lower inset), (d) Most of the lung sections show thin interalveolar septa (curved arrow) and some with thickened interalveolar septa (bifid arrow) with few focal areas of inflammatory cell infiltration (*). Most of the bronchiolar (B) epithelial lining are normal (↑) (upper inset). The alveoli are mostly lined by the thin type I pneumocyte (dot arrow) and pneumocytes type II (arrowhead) (lower inset), (e) Most of the bronchiolar (B) epithelial lining (↑) is normal as compared to that of the control group with a nearby blood vessel (v). Most of the alveoli (A) and alveolar sacs (s) show thin interalveolar septa (curved arrow) with few focal inflammatory cell infiltration (*) near the bronchiole. Most of the bronchiolar (B) epithelial lining are normal (↑) (upper inset). The alveoli are mostly lined by the thin type I pneumocyte (dot arrow) with their flat nuclei and pneumocytes type II (arrowhead) (Lower inset)

Biochemical results

Assessment of High Mobility Group Protein B1 (HMGB1) in lung tissue homogenate and in rats in different experimental groups: In the current study, HGMB1 in the lung homogenate was detected and summarized in (Table 1) and (Fig. 3a), the mean HGMB1 exhibited a significant increase in BLM untreated rats ($p<0.0001$) versus control rats and all experimental treated rats with PFD alone, agma alone and the combination of PFD and agma. The PFD ($p = 0.30$), agma ($p = 0.51$) and PFD+agma ($p = 0.55$) groups exhibited non-

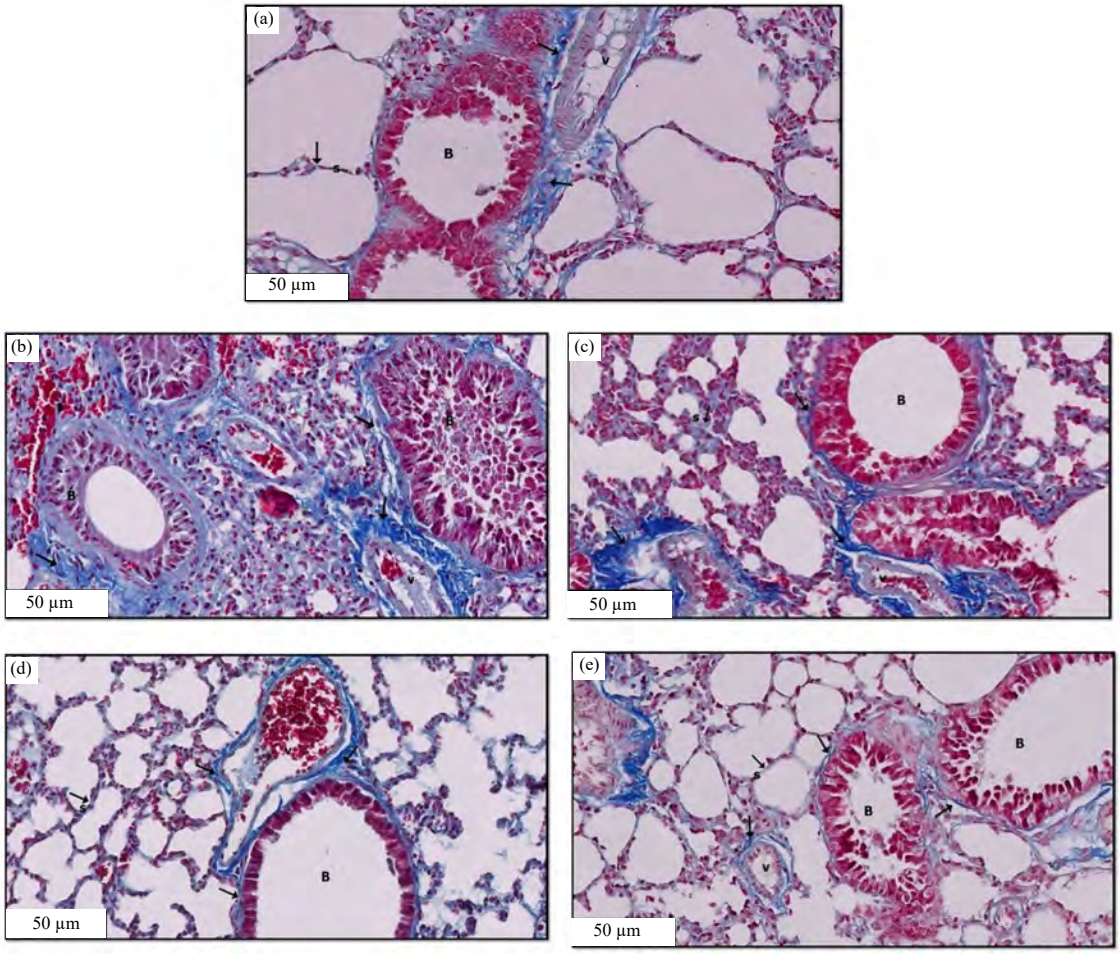

Fig. 2(a-e): Masson trichrome stained sections of a rat lung in different experimental groups after 28 days showing, (a) Control group, (b) Bleomycin group, (c) Bleomycin+pirfenidone (PFD), (d) Bleomycin+agma and (e) Bleomycin+PFD+agma

(a) Few collagen fibers (↑) in the interalveolar septa (s), around the bronchiole (B) and surrounding mainly the walls of the blood vessels (V) are seen, (b) Marked collagen fibers (↑) deposition in the interstitial tissue, bronchiole (B), and blood vessel (v) are seen, (c) Moderate collagen fibers (↑) in the interalveolar septa (s) and around the bronchiole (B), (d) Mild collagen fibers (↑) in the interalveolar septa (s) and around the bronchiole (B) are seen and (e) Few collagen fibers (↑) in the interalveolar septa (s), around the bronchiole (B), surrounding mainly the walls of the blood vessels (v) are seen, masson trichrome stain ×20 and scale bar 50 µm

significant from the control group. Interestingly, the PFD group and Agmatine group exhibited ns difference (p>0.99, p>0.99, respectively) of the mean HGMB1 as compared to the PFD+Agmatine.

Assessment of oxidative stress markers malondialdehyde, superoxide dismutase (SOD) and reduced glutathione in lung tissue homogenate and in rats in different experimental groups: In the current study, MDA in the lung homogenate was detected and summarized in Table 1 and Fig. 3b. The mean MDA exhibited a significant increase in BLM untreated rats (p<0.0001) versus control and all experimental treated rats with PFD alone, agma alone and the combination of PFD and agma. However, PFD (p = 0.99), agma (p>0.99) and PFD+agma (p = 0.97) exhibited no significant difference from the control group. Interestingly, the PFD and agma groups showed a non-significant difference (p = 0.94, p = 0.51, respectively) in the mean MDA versus the PFD+agma.

In the current study, SOD in the lung homogenate was detected and summarized in Table 1 and Fig. 3c. The mean SOD exhibited a significant (p<0.0001) decrease in BLM untreated rats in contrast with control rats and all experimental treated rats (PFD group, agma group and the combination of PFD and agma). However, there was no significance of the control group with the PFD group (p = 0.67), agma group (p>0.99) and PFD+agma (p = 0.99)

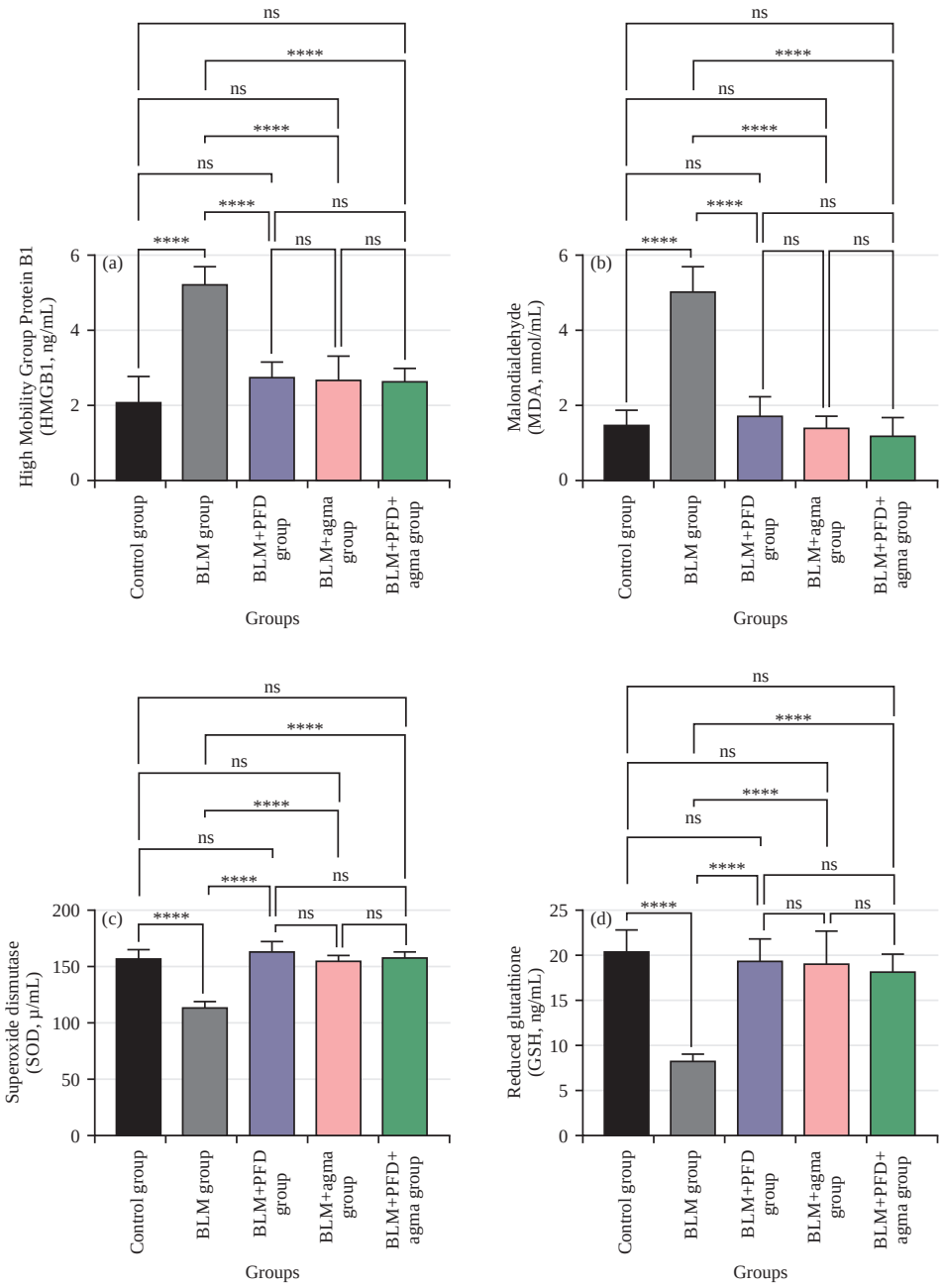

Fig. 3(a-d): Effect of Agmatine administration after 28 days on (a) High Mobility Group Protein B1 (HMGB1), (b) Malondialdehyde (MDA) (c) Superoxide dismutase (SOD) and (d) Reduced glutathione (GSH) on bleomycin induced chronic pulmonary fibrosis in rats in different experimental groups

Data are Mean±Standard Deviation (SD), One-way ANOVA followed by Tukey's multiple comparison test, n: Non-significant and ****p<0.0001

group. Interestingly, rats treated with PFD and agma alone showed a non-significant difference (p = 0.95, p = 0.99, respectively) of the mean SOD in contrast with the PFD+agma.

The GSH in the lung homogenate was detected and summarized in Table 1 and Fig. 3d, the mean GSH exhibited a significant (p<0.0001) decrease in BLM untreated rats in contrast with control rats and all experimental (PFD group, agma group and the combination of PFD and agma). However, there was no significant between control group and PFD group (p = 0.99), the agma group (p = 0.98) and the PFD+agma group (p = 0.76). Interestingly, the PFD group

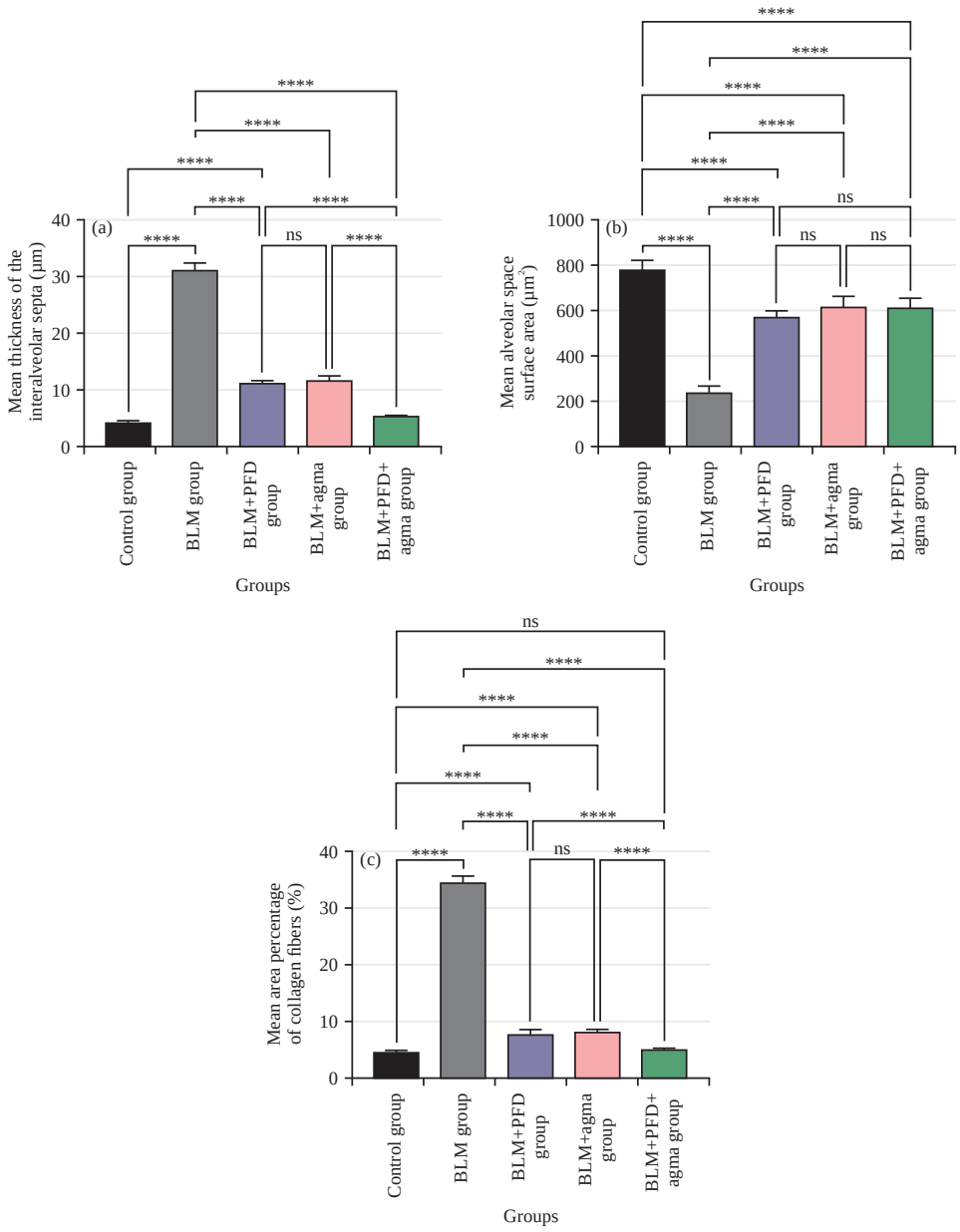

Fig. 4(a-c): Effect of agma administration after 28 days, (a) Mean thickness of the interalveolar septa in (µm), (b) Mean alveolar space surface area (µm2) and (c) Mean area percentage of collagen fibers (%) on bleomycin induced chronic pulmonary fibrosis in rats in different experimental groups

Data are Mean±Standard Deviation (SD), One-way ANOVA followed by Tukey's multiple comparison tests, ns: Non-significant and ****p<0.0001

(p = 0.99) and agma group (p = 0.99) showed a non-significant difference in the mean GSH in contrast with the PFD+agma.

Morphometric results

Mean thickness of the interalveolar septa (µm): As shown in Table 2 and Fig. 4a, the mean thickness of the interalveolar septa exhibited a significant (p<0.0001) decrease in contrast with all experimental groups BLM group, PFD group and agma group. However, when comparing the control group and the group that was given PFD and agma, there was no significant change (p = 0.93). Interestingly, rats treated group with PFD alone and agma alone showed a significant decrease (p<0.0001) in contrast with the BLM group and a significant comparing the BLM group treated with PFD alone to the BLM group treated with agma alone, there was no

Table 1: Effect of Agmatine administration after 28 days on the (A) (HGMB1, ng/mL), (B) (MDA, nmol/mL), (C) (SOD, µ/mL) and (D) (GSH, ng/mL) on bleomycin induced chronic pulmonary fibrosis in different experimental groups

	Biochemical results (Mean±SD)			
Groups (N = 6)	High Mobility Group Protein B1 (HGMB1, ng/mL)	Malondialdehyde (MDA, nmol/mL)	Superoxide dismutase (SOD, µ/mL)	Reduced Glutathione (GSH, ng/mL)
Control group	2.08±0.69	1.47±0.38	157.50±8.21	20.33±2.43
Bleomycin group	5.23±0.40[a]	5.03±0.63[a]	114.20±4.92[a]	8.28±0.65[a]
Bleomycin treated with pirfenidone group	2.76±0.36[b]	1.71±0.48[b]	164.50±8.80[b]	19.28±2.41[b]
Bleomycin treated with agma group	2.66±0.67[b]	1.39±0.31[b]	156.20±4.40[b]	19.03±3.56[b]
Bleomycin treated with pirfenidone and agma group	2.65±0.35[b]	1.20±0.48[b]	159.80±3.48[b]	18.20±1.86[b]

Values are Mean±Standard Deviation (SD), N: Number of animals, One-way ANOVA followed by Tukey's multiple comparison test, [a]p<0.05 in comparison to the control group and [b]p<0.05 in comparison to the bleomycin group

Table 2: Effect of agma administration after 28 days on the mean thickness of the interalveolar septa, alveolar space surface area and area percentage of collagen fibers on bleomycin-induced chronic pulmonary fibrosis in different experimental groups

	Morphometric results (Mean±SD)		
Groups (N = 6)	Mean thickness of the interalveolar septa in (µm)	Mean alveolar space surface area (µm^2)	Mean area percentage of collagen fibers (%)
Control group	4.20±0.82	782.8±42.38	4.65±0.32
Bleomycin group	31.21±3.08[a]	243.70±23.12[a]	34.57±1.18[a]
Bleomycin treated with pirfenidone group	11.10±1.09[a,b]	576.20±22.07[a,b]	7.83±0.92[a,b]
Bleomycin treated with agma group	11.62±1.56[a,b]	616.90±53.25[a,b]	8.16±0.52[a,b]
Bleomycin treated with pirfenidone and agma group	5.35±0.23[b,c,d]	613.60±46.53[a,b]	5.18±0.11[b,c,d]

Values are Mean±Standard Deviation (SD), N: Number of animals, One-way ANOVA followed by Tukey's multiple comparison test, [a]p<0.05 in comparison to the control group, [b]p<0.05 in comparison to the bleomycin group, [c]p<0.05 in comparison to the bleomycin group treated with pirfenidone and [d]p<0.05 in comparison to the bleomycin group treated with nintedanib

significant difference (p = 0.99). Notably, when comparing PFD+agma-treated rats to PFD-only-treated rats and agma-only-treated rats, there was a significant decrease (p<0.0001).

Mean alveolar space surface area (µm^2): Table 2 and Fig. 4b demonstrate a statistically significant (p<0.0001) decline in mean alveolar space surface area when comparing all experimental treated groups. Those who were given PFD, agma and a combination of PFD and agma were classified as experimental treated groups. Interestingly, the PFD and agma groups exhibited a significant decrease (p<0.0001) in contrast with the BLM group. Additionally, compared to the group given agma alone, the BLM rats who were given PFD alone exhibited no statistically significant change (p = 0.59). Interestingly, there was a non-significant difference (p = 0.70, p>0.99; respectively) between treated rats with PFD+agma in contrast with the PFD group and agma group.

Mean area percentage of collagen fibers (%): The mean area percentage of collagen fibers showed a significant (p<0.0001) decrease compared to all experimental groups BLM group, BLM treated with PFD and agma. Although p = 0.91 indicated no significant difference between the control group and the PFD+agma group. Interestingly, the PFD group and agma group showed a significant decrease (p<0.0001) in contrast with the BLM group and a significant increase (p<0.0001) in contrast with the control group. Moreover, the PFD group exhibited no significant (p = 0.99) difference in contrast with the agma group. Notably, when comparing PFD+agma-treated rats to PFD-only-treated rats and agma-only-treated rats, there was a significant decrease (p<0.0001) (Table 2 and Fig. 4c).

DISCUSSION

A chronic, progressive and ultimately fatal interstitial lung disease, pulmonary fibrosis has no known cause, a dismal prognosis and few treatment options. Among the most defining features of PF is the abnormal proliferation and activation of fibroblasts and myofibroblasts, which leads to an increase in ECM formation[31,32]. Much research has been done to demonstrate the possible medications for treating PF. However, only a small number of viable candidates are identified. Consequently, there is a pressing need for cutting-edge studies that can develop safe antifibrotic medicines. Marked degenerative changes of the lung appeared at different biochemical, histological as well as and morphometric levels occurred due to BLM. The results demonstrated that agma has potent anti-oxidative and antifibrotic effects against BLM-induced fibrosis in rats.

In this research, we used the gold standard for animal models of lung fibrosis, the BLM-induced PF rat model[33]. Despite lacking a suitable animal model of PF in humans, the BLM-induced model is well documented and shares several features with human disease[34]. When BLM is instilled intratracheally into an animal model, pulmonary harm occurs similarly to people, including an inflammatory response and fibrosis[35,36]. In addition, the prevalence of PF is higher in males than in females. Possible causes include X-linked genes that protect against PF and estrogens' protective effect on premenopausal women's collagen metabolism. Research also shows that male rats had a greater reactivity to bleomycin than female rats do and this is true across all ages of rats[37].

The histological results of this study confirmed the previously reported histological features of the BLM-induced rat model of PF, including extensive vacuolization of bronchiolar epithelial cells with pyknotic nuclei, alveolar obliteration and inflammatory cellular infiltrations, with significant collagen deposition in the lung tissues becoming most apparent on day 28. Current results corroborated previous studies indicating that BLM first triggers an acute inflammatory response (7-10 days after infection), which then gradually declines as fibrotic changes develop and persist (3-4 weeks)[4,8,10]. Furthermore, Zakaria *et al.*[30] revealed that the examination of H&E-stained sections from the BLM induced fibrosis group demonstrated a clear alteration of lung architecture, with significant thickening of the inter-alveolar septa and collapsed alveoli noted in a patchy distribution all through much of the lung tissue, 28 days after bleomycin administration.

Masson's trichrome staining showed that the BLM group had a greater mean area percentage of collagen fibers than the control group and all experimentally treated groups. This finding could be explained by BLM's capacity to enhance the proliferation of myofibroblasts. Consistent with this prior finding, Kulkarni *et al.*[38] discovered that BLM therapy dramatically induced overexpression of profibrotic genes, which are a crucial marker for myofibroblasts. Histomorphometry of trichrome-stained sections further verified induced lung fibrosis by demonstrating a considerably larger percentage area of collagen deposition in the induced fibrosis group compared to the control group[30]. According to research by Reinert *et al.*[39] and Kim *et al.*[40] BLM stimulates alveolar macrophages to produce inflammatory and profibrotic cytokines, including Interleukin-1 (IL-1), macrophage inflammatory protein-1 and others. Alveolar collapse and enhanced collagen deposition result from these cytokines' effects on fibroblast proliferation and activation. Despite this, the BLM response, which includes increased protein influx permeability and inflammatory cells, seems to be more likely associated with increased collagen synthesis. Thus, circulating mediators and mediators produced by resident lung cells or those that infiltrate lung tissues may come into contact with fibroblasts[40]. Pirfenidone (PFD) is an approved drug for PF treatment with antifibrotic, antioxidant and anti-inflammatory effects[41]. It inhibits the differentiation and proliferation of fibroblasts, the synthesis of collagen and the generation of inflammatory cytokines[42]. In the current study, we evaluated the effect of PFD alone or in combination with agma on PF and compared it with agma alone on day 28. The current study showed that PFD reduced BLM-induced alveolar damage, inflammatory cellular infiltrations, extravasation of RBCs and pulmonary fibrosis. The PFD-alone treated group and PFD+agma-treated group exhibited reduced inflammatory cell infiltration and collagen deposition, as opposed to the BLM group. This finding aligns with the results of a prior study[4,42]. Fikry *et al.*[4] found that the administration of PFD resulted in a notable decrease in the elevated levels of hydroxyproline, histological structures and Ashcroft and acute lung injury scores induced by BLM. These findings indicated that PFD has the potential to alleviate lung inflammation and fibrosis caused by BLM in mice, while also enhancing resistance to methylprednisolone. Additionally, the study revealed that rats fed with PFD exhibited a faster recovery from bleomycin-induced pulmonary fibrosis, with significantly reduced lung damage and fibrosis as evidenced by Masson's trichrome staining and the Ashcroft score 28 days after the initial injury.

To determine the mechanism(s) by which agma protects against BLM-induced PF, the current study assessed HGMB1, oxidative stress and histomorphometry alterations in lung tissue. Agmatine therapy may directly alleviate BLM treatment since the current study indicated that early treatment with agma therapy improved lung appearance. The H&E-stained sections showed increased collagen fibers density without significantly altering alveolar surface area or septal thickness, lending credence to this theory. This finding corroborated with the findings of El-Agamy *et al.*[21], who found that agma offers protection against silica-induced lung fibrosis. In addition, agma alleviates pulmonary edema and inflammation by preventing the formation of inflammatory cells and repairing histopathological damage. Agma's protective impact may stem from the amino acid's capacity to inhibit NO and TNF-generation while simultaneously lowering lipid peroxidation and increasing antioxidant status. This research supports using agma as a treatment option for pulmonary fibrosis.

Overproduction of ROS was already shown to be part of the rat lung response to BLM. In the midst of an inflammatory response, neutrophils release superoxide during a burst of respiration. The overproduction of ROS has significant pathophysiological implications due to its interactions with numerous cellular macromolecules[8]. As seen here, BLM led to elevated lung lipid peroxidation, as measured by malondialdehyde[14] concentration, a common marker of oxidative stress and antioxidant state[38,43]. With this came a precipitous drop in SOD and GSH activity. The levels of SOD and GSH were also elevated, but the MDA level was dramatically decreased after agma administration. Agmatine's capacity to scavenge free radicals and the resulting decrease in oxygen derivatives such as hydrogen peroxide was consistent with these findings[44,45]. Although agma's ability to inhibit NF-B activation in hyperglycemic mesangial cells or its ability to activate -2 adrenergic transmission in retinal ganglion cells have been hypothesized as potential mechanisms for its antioxidant benefits, they remain unproven[46,47]. As this study has shown, agma can potentially lessen the oxidative stress caused by the inflammatory response to BLM particles.

Research in the last few years has shown that HMGB1 activity is crucial for fibroblast proliferation, EMT and ultimately ECM deposition[12,13]. The current investigation demonstrated that pulmonary HMGB1 levels were dramatically upregulated following BLM treatment. On the other hand, agma therapy suppressed HMGB1 expression, indicating that agma's antifibrotic function is partly owed to its ability to prevent the release of HMGB1. Our findings suggest that agma's possible protective impact may be attributable, in part, to the fact that its effects on myofibroblast proliferation and extracellular matrix (ECM) deposition are blunted. Agma has recently been found to reduce pulmonary inflammation and oxidative stress[21]. Palumbo *et al.*[48] have demonstrated that extracellular HMGB1 and its receptor play a crucial role in the migration and proliferation of vessel-associated stem cells, potentially causative to muscle tissue regeneration. Anti-HMGB1 treatment holds promise in preventing lung injure and fibrosis through various mechanisms[48]. The proliferation of smooth muscle cells characterizes pulmonary fibrosis. Angiogenesis factors, including Vascular Endothelial Growth Factor (VEGF), Tumor Necrosis Factor-Alpha (TNF-α) and Interleukin-8 (IL-8), are known to be produced by activated macrophages, which HMGB1 is known to do[49]. Endothelial cell migration and sprouting were shown to be stimulated by exogenous HMGB1 *in vitro* by Schlueter *et al.*[50] in a dose-dependent manner. The etiology of BLM-induced PF was revealed to involve angiogenesis[51]. Thirdly, Dumitriu *et al.*[52] showed that activated dendritic cells secrete their HMGB1 and drive dendritic cell maturation. The T cell maintenance and expansion depend on dendritic cell maturation. There is some debate about whether or not T cells contribute to lung damage and fibrosis, although anti-HMGB1 medication may mitigate this scenario by suppressing T cell activation.

CONCLUSION

Agmatine, combined with PFD, was shown to reduce the severity of BLM-induced histological and biochemical alterations in rat lungs without completely reversing them. Agmatine's anti-inflammatory and antioxidant capabilities and ability to scavenge for free radicals in action may account for this. However due to the side effects of Agmatine, these results cannot be readily translated into clinical applications.

SIGNIFICANCE STATEMENT

The purpose of the study was to examine if Agmatine (agma) alone or in combination with pirfenidone (PFD) could have a protective effect on pulmonary fibrosis induced by bleomycin (BLM) in a rat model. According to the study, the combination of Agmatine and PFD reduced the severity of histological and biochemical changes induced by BLM in rat lungs, but did not completely reverse them. The groups that received the treatment showed a significant decrease in HMGP1 and MDA levels compared to the BLM group, as well as a significant increase in SOD and GSH levels. These results offer promising therapeutic options for the management of pulmonary fibrosis. Future studies could investigate the therapeutic effects of Agmatine and pirfenidone on pulmonary fibrosis in humans, as well as their potential use in combination with other therapies. Understanding the disease's underlying mechanisms, such as uncontrolled fibroblast proliferation and excessive production of extracellular matrix (ECM) proteins, is crucial for developing effective treatments.

ACKNOWLEDGMENT

The author is thankful to the Deanship of Scientific Research of Najran University for funding this work through grant research code NU/NRP/MRC/12/1.

REFERENCES

1. Sime, P.J. and K.M.A. O'Reilly, 2001. Fibrosis of the lung and other tissues: New concepts in pathogenesis and treatment. Clin. Immunol., 99: 308-319.

2. Warsinske, H.C., A.K. Wheaton, K.K. Kim, J.J. Linderman, B.B. Moore and D.E. Kirschner, 2016. Computational modeling predicts simultaneous targeting of fibroblasts and epithelial cells is necessary for treatment of pulmonary fibrosis. Front. Pharmacol., Vol. 7. 10.3389/fphar.2016.00183.
3. Zhou, Y., Z. He, Y. Gao, R. Zheng, X. Zhang, L. Zhao and M. Tan, 2016. Induced pluripotent stem cells inhibit bleomycin-induced pulmonary fibrosis in mice through suppressing TGF-β1/smad-mediated epithelial to mesenchymal transition. Front. Pharmacol., Vol. 7. 10.3389/fphar.2016.00430.
4. Fikry, H., L.A. Saleh and S. Abdel Gawad, 2022. Therapeutic effect of adipose-derived mesenchymal stem cells (AD-MSCs) compared to pirfenidone on corticosteroid resistance in a mouse model of acute exacerbation of idiopathic pulmonary fibrosis. Histol. Histopathol., 37: 1065-1083.
5. Demirkol, B., Ş. Gül, M. Çörtük, N.A. Fener and E. Yavuzsan *et al*., 2023. Protective efficacy of pirfenidone in rats with pulmonary fibrosis induced by bleomycin. Sarcoidosis Vasculitis Diffuse Lung Dis., Vol. 40. 10.36141/svdld.v40i3.13847.
6. Khan, M.A., N. Sherbini, S. Alyami, A. Al-Harbi, M. Al-Ghamdi, S. Alrajhi and R. Rajendram, 2023. Nintedanib and pirfenidone for idiopathic pulmonary fibrosis in King Abdulaziz Medical City, Riyadh: Real-life data. Ann. Thoracic Med., 18: 45-51.
7. Sgalla, G., B. Iovene, M. Calvello, M. Ori, F. Varone and L. Richeldi, 2018. Idiopathic pulmonary fibrosis: Pathogenesis and management. Respir. Res., Vol. 19. 10.1186/s12931-018-0730-2.
8. Zaghloul, M.S., R.A. Abdel-Salam, E. Said, G.M. Suddek and H.A.R. Salem, 2017. Attenuation of bleomycin-induced pulmonary fibrosis in rats by flavocoxid treatment. Egypt. J. Basic Appl. Sci., 4: 256-263.
9. Liu, T., F.G. de Los Santos and S.H. Phan, 2017. The Bleomycin Model of Pulmonary Fibrosis. In: Fibrosis: Methods and Protocols, Rittié, L. (Ed.), Humana Press, New York, ISBN: 978-1-4939-7113-8, pp: 27-42.
10. Mouratis, M.A. and V. Aidinis, 2011. Modeling pulmonary fibrosis with bleomycin. Curr. Opin. Pulm. Med., 17: 355-361.
11. Cai, J., J. Wen, E. Bauer, H. Zhong, H. Yuan and A.F. Chen, 2015. The role of HMGB1 in cardiovascular biology: Danger signals. Antioxid. Redox Signaling, 23: 1351-1369.
12. Li, L.C., D.L. Li, L. Xu, X.T. Mo and W.H. Cui *et al*., 2015. High-mobility group Box 1 mediates epithelial-to-mesenchymal transition in pulmonary fibrosis involving transforming growth factor-*β*1/Smad2/3 signaling. J. Pharmacol. Exp. Ther., 354: 302-309.
13. Hamada, N., T. Maeyama, T. Kawaguchi, M. Yoshimi and J. Fukumoto *et al*., 2008. The role of high mobility group Box1 in pulmonary fibrosis. Am. J. Respir. Cell. Mol. Biol., 39: 440-447.
14. Kotagale, N.R., B.G. Taksande and N.N. Inamdar, 2019. Neuroprotective offerings by agmatine. NeuroToxicology, 73: 228-245.
15. Akasaka, N. and S. Fujiwara, 2020. The therapeutic and nutraceutical potential of agmatine, and its enhanced production using *Aspergillus oryzae*. Amino Acids, 52: 181-197.
16. Kwon, E.J. and M.M. Kim, 2017. Agmatine modulates melanogenesis via MITF signaling pathway. Environ. Toxicol. Pharmacol., 49: 124-130.
17. Hong, S., C.Y. Kim, J.E. Lee and G.J. Seong, 2009. Agmatine protects cultured retinal ganglion cells from tumor necrosis factor-alpha-induced apoptosis. Life Sci., 84: 28-32.
18. Uzbay, T.I., 2012. The pharmacological importance of agmatine in the brain. Neurosci. Biobehav. Rev., 36: 502-519.
19. Su, R.B., X.L. Wei, J.Q. Zheng, Y. Liu, X.Q. Lu and J. Li, 2004. Anticonvulsive effect of agmatine in mice. Pharmacol. Biochem. Behav., 77: 345-349.
20. Zomkowski, A.D.E., L. Hammes, J. Lin, J.B. Calixto, A.R.S. Santos and A.L.S. Rodrigues, 2002. Agmatine produces antidepressant-like effects in two models of depression in mice. Neuroreport, 13: 387-391.
21. El-Agamy, D.S., M.H. Sharawy and E.M. Ammar, 2014. Agmatine attenuates silica-induced pulmonary fibrosis. Hum. Exp. Toxicol., 33: 650-660.
22. Gao, L., D. Jiang, J. Geng, R. Dong and H. Dai, 2019. Hydrogen inhalation attenuated bleomycin-induced pulmonary fibrosis by inhibiting transforming growth factor-β1 and relevant oxidative stress and epithelial-to-mesenchymal transition. Exp. Physiol., 104: 1942-1951.
23. Song, X., W. Yu and F. Guo, 2018. Pirfenidone suppresses bleomycin-induced pulmonary fibrosis and periostin expression in rats. Exp. Ther. Med., 16: 1800-1806.
24. Kmiec, Z., 2016. J.A. Kiernan. Histological and histochemical methods: Theory and practice. 5th edition, scion publishing, 2015, 571 pp. Folia Histochem. Cytobiol., 54: 58-59.
25. Yamada, S., K. Inoue, K. Yakabe, H. Imaizumi and I. Maruyama, 2003. High mobility group protein 1 (HMGB1) quantified by ELISA with a monoclonal antibody that does not cross-react with HMGB2. Clin. Chem., 49: 1535-1537.
26. Satoh, K., 1978. Serum lipid peroxide in cerebrovascular disorders determined by a new colorimetric method. Clin. Chim. Acta, 90: 37-43.
27. Nishikimi, M., N.A. Rao and K. Yagi, 1972. The occurrence of superoxide anion in the reaction of reduced phenazine methosulfate and molecular oxygen. Biochem. Biophys. Res. Commun., 46: 849-854.
28. Giustarini, D., P. Fanti, E. Matteucci and R. Rossi, 2014. Micro-method for the determination of glutathione in human blood. J. Chromatogr. B, 964: 191-194.
29. Albanawany, N.M., D.M. Samy, N. Zahran, R.M. El-Moslemany, S.M. Elsawy and M.W. Abou Nazel, 2022. Histopathological, physiological and biochemical assessment of resveratrol nanocapsules efficacy in bleomycin-induced acute and chronic lung injury in rats. Drug Delivery, 29: 2592-2608.

30. Zakaria, D.M., N.M. Zahran, S.A.A. Arafa, R.A. Mehanna and R.A. Abdel-Moneim, 2021. Histological and physiological studies of the effect of bone marrow-derived mesenchymal stem cells on bleomycin induced lung fibrosis in adult albino rats. Tissue Eng. Regener. Med., 18: 127-141.
31. Pardo, A. and M. Selman, 2016. Lung fibroblasts, aging, and idiopathic pulmonary fibrosis. Ann. Am. Thoracic Soc., 13: S417-S421.
32. Kendall, R.T. and C.A. Feghali-Bostwick, 2014. Fibroblasts in fibrosis: Novel roles and mediators. Front. Pharmacol., Vol. 5. 10.3389/fphar.2014.00123.
33. Jenkins, R.G., B.B. Moore, R.C. Chambers, O. Eickelberg and M. Königshoff *et al*., 2017. An official American thoracic society workshop report: Use of animal models for the preclinical assessment of potential therapies for pulmonary fibrosis. Am. J. Respir. Cell. Mol. Biol., 56: 667-679.
34. Calaway, A.C., R.S. Foster, N. Adra, T.A. Masterson and C. Albany *et al*., 2018. Risk of bleomycin-related pulmonary toxicities and operative morbidity after postchemotherapy retroperitoneal lymph node dissection in patients with good-risk germ cell tumors. J. Clin. Oncol., 36: 2950-2954.
35. Zhao, L., B. Mu, R. Zhou, Y. Cheng and C. Huang, 2019. Iguratimod ameliorates bleomycin-induced alveolar inflammation and pulmonary fibrosis in mice by suppressing expression of matrix metalloproteinase-9. Int. J. Rheum. Dis., 22: 686-694.
36. Williamson, J.D., L.R. Sadofsky and S.P. Hart, 2015. The pathogenesis of bleomycin-induced lung injury in animals and its applicability to human idiopathic pulmonary fibrosis. Exp. Lung Res., 41: 57-73.
37. Garate-Carrillo, A., J. Gonzalez, G. Ceballos, I. Ramirez-Sanchez and F. Villarreal, 2020. Sex related differences in the pathogenesis of organ fibrosis. Transl. Res., 222: 41-55.
38. Kulkarni, A.A., T.H. Thatcher, H.M. Hsiao, K.C. Olsen and R.M. Kottmann *et al*., 2013. The triterpenoid CDDO-Me inhibits bleomycin-induced lung inflammation and fibrosis. PLoS ONE, Vol. 8. 10.1371/journal.pone.0063798.
39. Reinert, T., C.S. da Rocha Baldotto, F.A.P. Nunes and A.A. de Souza Scheliga, 2013. Bleomycin-induced lung injury. J. Cancer Res., Vol. 2013. 10.1155/2013/480608.
40. Kim, M.S., A.R. Baek, J.H. Lee, A.S. Jang, D.J. Kim, S.S. Chin and S.W. Park, 2019. IL-37 attenuates lung fibrosis by inducing autophagy and regulating TGF-β1 production in mice. J. Immunol., 203: 2265-2275.
41. Puglisi, S., S.E. Torrisi, V. Vindigni, R. Giuliano, S. Palmucci, M. Mulè and C. Vancheri, 2016. New perspectives on management of idiopathic pulmonary fibrosis. Ther. Adv. Chronic Dis., 7: 108-120.
42. Liu, Y., F. Lu, L. Kang, Z. Wang and Y. Wang, 2017. Pirfenidone attenuates bleomycin-induced pulmonary fibrosis in mice by regulating Nrf2/Bach1 equilibrium. BMC Pulm. Med., Vol. 17. 10.1186/s12890-017-0405-7.
43. Sogut, S., H. Ozyurt, F. Armutcu, L. Kart and M. Iraz *et al*., 2004. Erdosteine prevents bleomycin-induced pulmonary fibrosis in rats. Eur. J. Pharmacol., 494: 213-220.
44. Quan, Y., J. Du and X. Wang, 2007. High glucose stimulates GRO secretion from rat microglia via ROS, PKC, and NF-κB pathways. J. Neurosci. Res., 85: 3150-3159.
45. Lee, W.T., S. Hong, S.H. Yoon, J.H. Kim, K.A. Park, G.J. Seong and J.E. Lee, 2009. Neuroprotective effects of agmatine on oxygen-glucose deprived primary-cultured astrocytes and nuclear translocation of nuclear factor-kappa B. Brain Res., 1281: 64-70.
46. Lee, G.T., H.J. Ha, H.C. Lee and Y.D. Cho, 2003. Agmatine reduces hydrogen peroxide in mesangial cells under high glucose conditions. BMB Rep., 36: 251-257.
47. Iizuka, Y., S. Hong, C.Y. Kim, W.I. Yang, J.E. Lee and G.J. Seong, 2010. Protective mechanism of agmatine pretreatment on RGC-5 cells injured by oxidative stress. Braz. J. Med. Biol. Res., 43: 356-358.
48. Palumbo, R., M. Sampaolesi, F. de Marchis, R. Tonlorenzi and S. Colombetti *et al*., 2004. Extracellular HMGB1, a signal of tissue damage, induces mesoangioblast migration and proliferation. J. Cell. Biol., 164: 441-449.
49. Andersson, U., H. Erlandsson-Harris, H. Yang and K.J. Tracey, 2002. HMGB1 as a DNA-binding cytokine. J. Leukocyte Biol., 72: 1084-1091.
50. Schlueter, C., H. Weber, B. Meyer, P. Rogalla, K. Röser, S. Hauke and J. Bullerdiek, 2005. Angiogenetic signaling through hypoxia: HMGB1: An angiogenetic switch molecule. Am. J. Pathol., 166: 1259-1263.
51. Derseh, H.B., K.U.E. Perera, S.N.V. Dewage, A. Stent and E. Koumoundouros *et al*., 2021. Tetrathiomolybdate treatment attenuates bleomycin-induced angiogenesis and lung pathology in a sheep model of pulmonary fibrosis. Front. Pharmacol., Vol. 12. 10.3389/fphar.2021.700902.
52. Dumitriu, I.E., P. Baruah, B. Valentinis, R.E. Voll and M. Herrmann *et al*., 2005. Release of high mobility group Box 1 by dendritic cells controls t cell activation via the receptor for advanced glycation end products. J. Immunol., 174: 7506-7515.